

Analogue saturation limit of single and double 10 mm microchannel plate photomultiplier tubes

J. S. Miines, T. M. Conneely, and C. J. Horsfield

Citation: [Review of Scientific Instruments](#) **87**, 11D832 (2016); doi: 10.1063/1.4961279

View online: <http://dx.doi.org/10.1063/1.4961279>

View Table of Contents: <http://scitation.aip.org/content/aip/journal/rsi/87/11?ver=pdfcov>

Published by the [AIP Publishing](#)

Articles you may be interested in

[Improved time response for large area microchannel plate photomultiplier tubes in fusion diagnostics](#)
Rev. Sci. Instrum. **85**, 11E601 (2014); 10.1063/1.4886759

[Applications of the Microchannel Plate for Mass Spectrometry](#)
AIP Conf. Proc. **991**, 82 (2008); 10.1063/1.2905143

[Operating a triple stack microchannel plate-phosphor assembly for single particle counting in the 12 – 300 K temperature range](#)
Rev. Sci. Instrum. **78**, 113301 (2007); 10.1063/1.2814030

[Gated Microchannel Plate Photomultipliers For Longitudinal Beam Diagnostics](#)
AIP Conf. Proc. **868**, 262 (2006); 10.1063/1.2401413

[True constant fraction trigger circuit for picosecond photon-timing with ultrafast microchannel plate photomultipliers](#)
Rev. Sci. Instrum. **68**, 2228 (1997); 10.1063/1.1148074

PHYSICS
TODAY

Welcome to a

Smarter Search 

with the redesigned
Physics Today Buyer's Guide

Find the tools you're looking for today!

Analogue saturation limit of single and double 10 mm microchannel plate photomultiplier tubes

J. S. Milnes,^{1,a)} T. M. Conneely,¹ and C. J. Horsfield²

¹Photek Ltd., 26 Castleham Road, St Leonards on Sea, East Sussex TN38 9NS, United Kingdom

²AWE Aldermaston, Reading, Berkshire RG7 4PR, United Kingdom

(Presented 7 June 2016; received 5 June 2016; accepted 1 August 2016;
 published online 2 September 2016)

Photek are a well-established supplier of microchannel plate (MCP) photomultiplier tubes (PMTs) to the inertial confinement fusion community. The analogue signals produced at the major inertial confinement fusion facilities cover many orders of magnitude, therefore understanding the upper saturation limit of MCP-PMTs to large low rate signals takes on a high importance. Here we present a study of a single and a double MCP-PMT with 10 mm diameter active area. The saturation was studied for a range of optical pulse widths from 4 ns to 100 ns and at a range of electron gain values: 10^3 to 10^4 for the single and 10^4 to 10^6 for the double. We have shown that the saturation level of ~ 1.2 nC depends only on the integrated charge of the pulse and is independent of pulse width and gain over this range, but that the level of charge available in deep saturation is proportional to the operating gain. *Published by AIP Publishing.* [<http://dx.doi.org/10.1063/1.4961279>]

I. INTRODUCTION

In a market that includes alternatives from Hamamatsu¹ and Photonis,² Photek are considered a well-established supplier of microchannel plate (MCP) photomultiplier tubes (PMTs) to the inertial confinement fusion (ICF) community. We have several detectors installed at NIF, Omega (LLE Rochester), and Orion (AWE). The MCP-PMTs produced by Photek have the shortest response time recorded by devices of this type with a small area single MCP PMT having a FWHM of ~ 85 ps,³ and in recent years Photek have also made significant improvements to their gating ability.⁴ The two main diagnostics where these detectors are used are gamma detection⁵ (in combination with a Cherenkov radiator) and neutron time of flight⁶ (in combination with a scintillator). Both of these diagnostics produce multi-photon pulsed signals that cover many orders of magnitude and often need multiple detectors operating at different levels of electron gain. As such, understanding the upper saturation limit of MCP-PMTs takes on a high importance as it is key to know the limitations of the whole diagnostic. Here we present a study of a single (PMT110) and a double (PMT210) MCP-PMT with 10 mm diameter active area. The saturation was studied for a range of optical pulse widths from 4 ns to 100 ns and at a range of electron gain values: 10^3 to 10^4 for the PMT110 and 10^4 to 10^6 for the PMT210.

II. EXPERIMENT

Measuring the saturation limit of a photo detector to pulsed signals should be simple: Linearly increase the

magnitude of the optical pulse input and monitor the electrical pulse output, and once this relationship becomes non-linear, the saturation is reached. In reality it is often difficult to control the accuracy of the optical input and can involve many time-consuming calibrations of light sources and neutral density (ND) filters, which posed a problem for this study as we wanted to look at a broad range of pulse amplitudes at multiple pulse widths which needed a level of automation and a reasonably simple setup.

To circumvent this issue and allow a level of automation into the experiment, we devised a system where the input optical pulse could be monitored at each and every setting by a separate photodetector known to be linear over this range, as shown on Fig. 1. The photodiode was a 10 mm diameter Photek PD010, essentially the same construction as the two PMTs under analysis but without the limited dynamic range that comes with using an MCP. Its linearity was confirmed by measuring the integrated pulse output up to the maximum value used at the limits of the pulse width (~ 200 pC at 4 ns and ~ 8 nC at 100 ns), and then making the same measurement but with 10% of the light simply by adding an ND of 1.0. Graphing the 10% range against the 100% range at both pulse widths produced good linear relationships.

At each data point the oscilloscope averaged the signal for 100 times to remove the natural signal variation caused by the limited number of photons per pulse, and then integrated the pulses to produce a charge value: Each data point thus consisted of the integrated charge of the signal pulse from the photodiode and the same from the PMT being analyzed. The ND filters were adjusted to suit the PMT gain and the level of saturation being measured, and the diffuser ensured a flat field at the detector input. The pulse width and amplitude of the laser diode pulses were controlled by a software script that also read out the charge values from the oscilloscope.

For all of the saturation curves shown in this study, the integrated charge from the photodiode reference pulse used on

Note: Contributed paper, published as part of the Proceedings of the 21st Topical Conference on High-Temperature Plasma Diagnostics, Madison, Wisconsin, USA, June 2016.

^{a)}Author to whom correspondence should be addressed. Electronic mail: james.milnes@photek.co.uk.

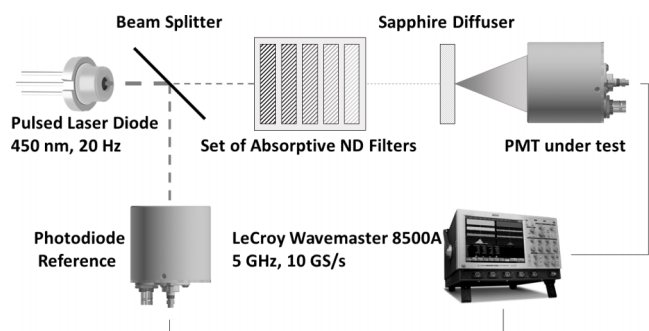


FIG. 1. Experimental layout for the PMT saturation study.

the x-axis is purely arbitrary as it only represents a fixed ratio of the light arriving at the photodiode and PMT, respectively. This ratio is set by the ND filters, which was altered to suit the experimental parameters of each experiment (pulse width, gain, level of saturation). The x-axis only serves to have a linear reference to compare, and the key parameter to take from each graph is the shape of the curve and the amount of charge produced by the PMT where the curve begins to show a non-linear relationship.

III. SATURATION CURVE

An example of a typical saturation curve is shown in Fig. 2, in this case for a PMT210 operating at a gain of 13 000

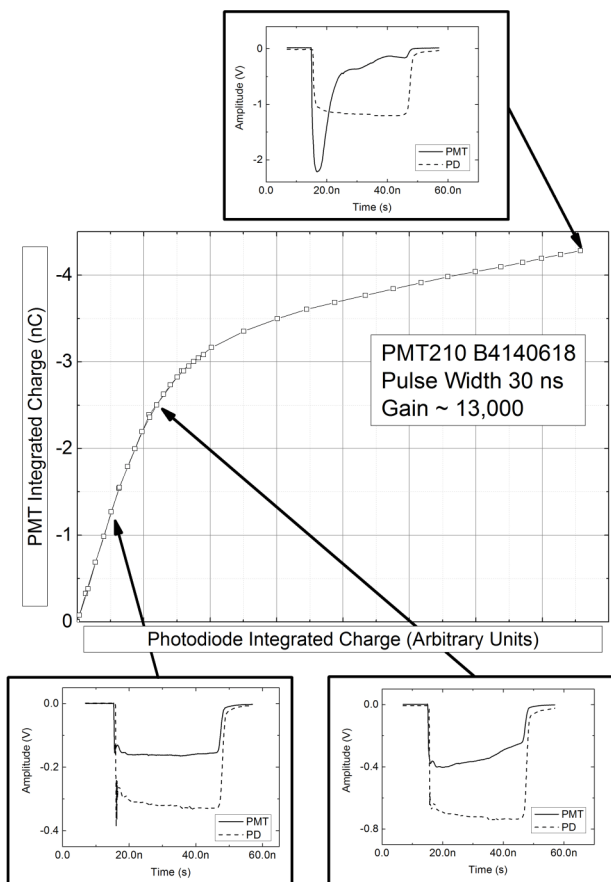


FIG. 2. Typical saturation curve for an MCP-PMT, with examples of the pulse shapes at various levels of saturation.

and an optical pulse width of 30 ns. At three points on the curve we have shown the resulting PMT and PD pulse shapes to illustrate how the saturation effect appears. At an output pulse charge of 1.3 nC, saturation first becomes noticeable due to the slight difference in pulse shape between the outputs of the PMT and the photodiode, which can be considered to show the true output of the laser diode. A slight dip at the end of the square pulse indicates the beginning of saturation and therefore the end of the linear region. As the magnitude of the optical pulse is increased the saturation becomes more evident, as shown at 2.5 nC, although it is only at this point that the curve becomes noticeably non-linear. Once the output reaches 4.3 nC, the PMT is clearly in deep saturation and the output pulse barely resembles the square input as shown by the pulse of the photodiode.

IV. PULSE WIDTH VARIATION

The first result of note was the lack of dependence between the shape of the saturation curve and the pulse width, an example of which is shown in Fig. 3 for a PMT110 operating at a gain of 12 500. Each set of curves was taken at different ND settings so the ratio of light reaching the PMT and the photodiode would be different, so they cannot be compared on the same graph. However, we measured the pulse widths of 10 ns and 30 ns in multiple sets to show that the curve shape was consistent across all pulse widths. Both PMT110 and PMT210 showed this effect over the full range of gain values and the same range of optical pulse widths, and the end of their linear regions is about 1.2 nC of integrated charge in the output pulse regardless of pulse width or gain.

V. GAIN VARIATION

Whilst the onset of non-linearity appears unaffected by the pulse width or gain, there is an effect on the shape of the saturation curve when the electron gain is altered. Taking the saturation curves for a pulse width of 10 ns for both devices, and then adjusting the arbitrary x-scale so that the linear regions overlap, we can see that the amount of charge produced when the PMT is in deep saturation increases when the PMT is operated at a higher gain, see Fig. 4. It is important to note, however, that the saturation curves only separate once the PMT is significantly outside of the linear region, so it should not be misinterpreted as extending the linear response of the PMT.

VI. DISCUSSION

This analysis confirms the assumption made in previous studies of MCP saturation in a low rate, multi-photon environment (as opposed to a high-rate, single photon regime) that looked at saturation in an MCP-based image intensifier from Proxivision.⁷ The assumption was that any saturation would result in a signal depression independent of the pulse

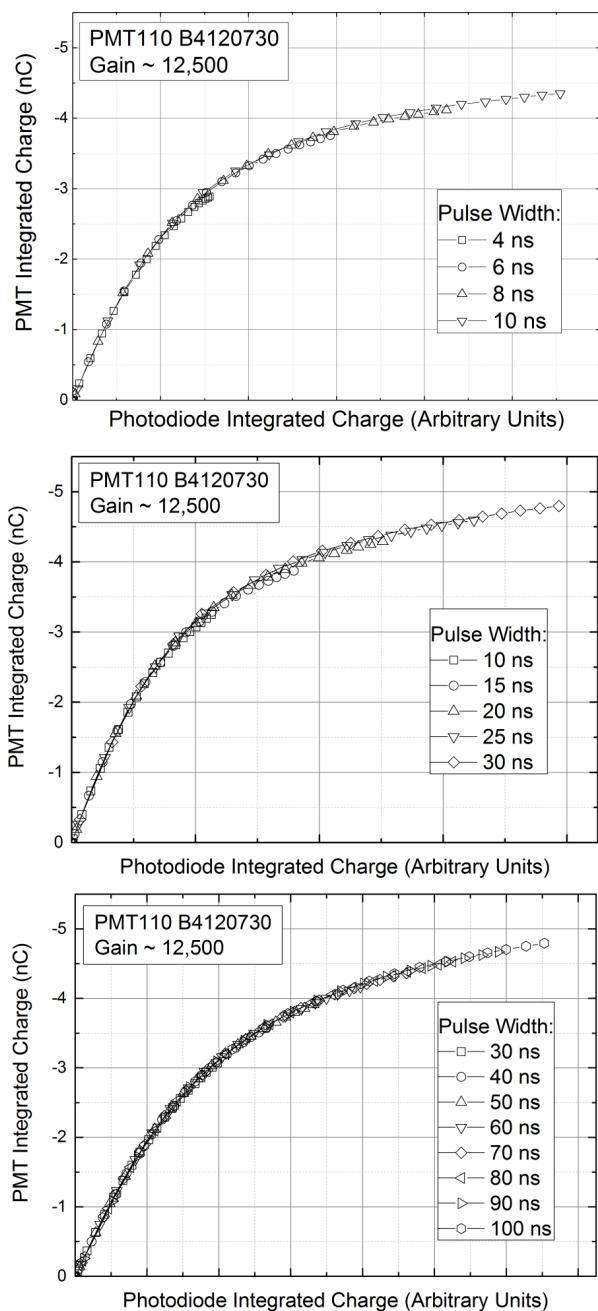


FIG. 3. Saturation curves of a PMT110 operating at a gain of 12 500 showing the absence of any dependence between the shape of the curve and optical pulse widths for the range 4 ns–100 ns.

width, provided it is significantly shorter than the recharge time of the MCP, which is in the order of milliseconds, and is also suggested by a modelling analysis.⁸ Both of these studies indicate a continued increase in signal output up to a level considerably beyond the linear region. They suggest that this is due to the beginning of saturation occurring at the end of the MCP pore, while the rest of the pore remains unsaturated. Therefore, even though the end of the pore may only be operating at a gain near unity, there is still scope for the rest of the pore to produce more electron signals if asked. It is also proposed that an MCP operating at a higher gain level is able to produce more signals when saturated simply due to the extra charge stored in the capacitance of the MCP

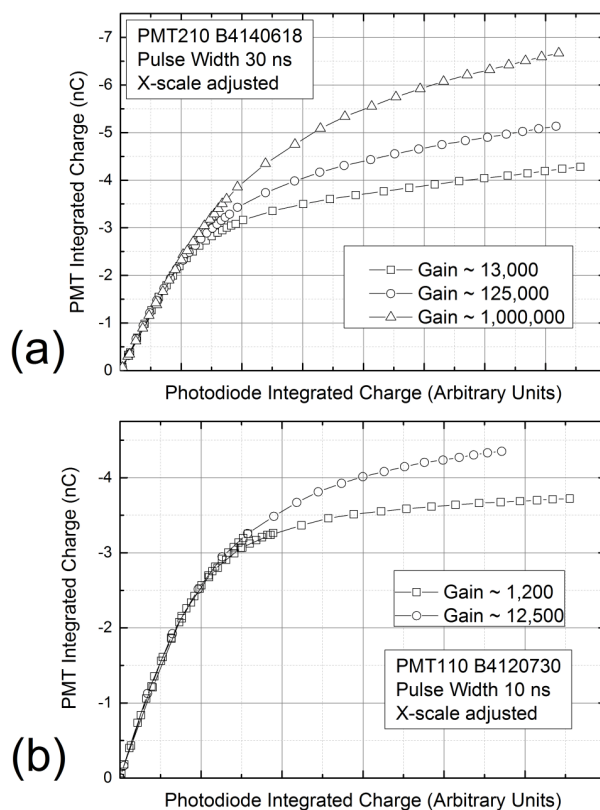


FIG. 4. Typical saturation curves at a range of electron gain values for (a) a PMT210 and (b) a PMT110 using a 10 ns optical pulse input. In both the figures the arbitrary x-scale was adjusted to overlap the linear region.

as more voltage would be applied across it, which is observed in the results of this study.

VII. CONCLUSION

We have measured the pulsed saturation curves of a single and a double 10 mm MCP-PMT over their respective working gain ranges and over a range of pulse widths between 4 ns and 100 ns. We have shown that the saturation level of ~1.2 nC depends only on the integrated charge of the pulse and is independent of pulse width and gain over this range. The level of charge available in deep saturation is proportional to the operating gain; however, this does not extend the linear region of either device.

¹Hamamatsu Photonics K. K., Photomultiplier Tubes and Related Products, revised February 2016.
²See <https://www.photonis.com/en/product/mcp-pmt> for details of the Photonis MCP-PMT model.
³J. S. Milnes, T. M. Conneely, and J. R. Howorth, in Proceedings of the 1st EPS Conference on Plasma Diagnostics, 2015, PoS(ECPD2015)005.
⁴J. S. Milnes, C. J. Horsfield, M. S. Rubery, V. Yu Glebov, and H. W. Herrmann, *Rev. Sci. Instrum.* **83**, 10D301 (2012).
⁵J. M. Mack, R. R. Berggren, S. E. Caldwell, S. C. Evans, J. R. Faulkner, Jr., R. A. Lerche, J. A. Oertel, and C. S. Young, *Nucl. Instrum. Methods Phys. Res., Sect. A* **513**, 566–572 (2003).
⁶C. J. Forrest, P. B. Radha, V. Yu Glebov, V. N. Goncharov, J. P. Knauer, A. Pruyne, M. Romanofsky, T. C. Sangster, M. J. Shoup, C. Stoeckl, D. T. Casey, M. Gatu-Johnson, and S. Gardner, *Rev. Sci. Instrum.* **83**, 10D919 (2012).
⁷D. Fastje, H. B. Barber, V. Bora, D. Lemieux, B. Miller, and G. P. Grim, *Proc. SPIE* **8854**, 88540J (2013).
⁸L. Giudicotti, *Nucl. Instrum. Methods Phys. Res., Sect. A* **659**, 336–347 (2011).